

# Preparation and CO<sub>2</sub> Adsorption Performance of Porous Aluminum Fumarate MOFs Pellet

Lijiao Ma, Yudong Ding\*, Fengqi Zeng, Xingxing Zhao, Qiang Liao, Hong Wang, Xun Zhu

Chongqing Univ., Key Laboratory of Low-grade Energy Utilization Technologies and Systems, Shazheng St.174, Shapingba Dist., Chongqing 400030, China  
 dingyudong@cqu.edu.cn

Aluminum fumarate metal organic frameworks (AlFu MOFs) pellet was successfully prepared with outstanding porous structure and its CO<sub>2</sub> adsorption performance was investigated. As the binder mass increased, the pellet mechanical strength rose while the CO<sub>2</sub> adsorption capacity reduced. The chosen AlFu pellet with 2.5wt% carboxymethyl cellulose sodium (CMC) binder retained the micro-morphology characteristics with a specific surface area of 726.06 m<sup>2</sup>/g and micropore volume of 0.33 cm<sup>3</sup>/g. The adsorption performance of CO<sub>2</sub> by the pellets was studied at different partial pressures and temperatures. The results showed that the adsorption capacity of CO<sub>2</sub> in AlFu pellet was increased with lower adsorption temperature and higher CO<sub>2</sub> partial pressure, the maximum adsorption amount was 1.26 mmol/g at 35 °C and 1.0 bar. The CO<sub>2</sub> adsorption kinetics and the limiting factors for adsorption rate were analyzed. Compared with pseudo-second order model the pseudo-first order kinetic model can better describe the CO<sub>2</sub> physical adsorption behavior of AlFu pellet. The rate-limiting kinetic analysis revealed that the CO<sub>2</sub> adsorption rate was determined by film diffusion and intra-particle diffusion rather than inter-particle diffusion.

## 1. Introduction

CO<sub>2</sub> capture and storage (CCS) technology is a vital approach for reducing CO<sub>2</sub> emission effectively, therefore efficient and economical absorbent plays an important role (Ding et al., 2019). The solid adsorption method is commonly adopted with simple process and low energy consumption for adsorbing CO<sub>2</sub>. AlFu is a kind of porous MOFs material, which is one-dimensional pore structure by the combination of aluminum ions and fumarate ions. Because of the porosity (Teo et al., 2017) and unique hydrothermal stability (Jeremias et al., 2014), AlFu as a promising adsorbent has been universally applied in many fields, such as fluoride removal from water (Karmakar et al., 2016), CH<sub>4</sub> capture from emission (Sadiq et al., 2018) and CO<sub>2</sub> capture from flue gas. Coelho et al. (2016) analyzed the impact of water on CO<sub>2</sub> adsorption performance and received the adsorption heat. Dundar et al. (2017) obtained Henry's adsorption constants, adsorption enthalpies and adsorption entropies by configurational bias Monte Carlo simulation. It provided additional methods and comprehensive parameters for the performance assessment.

The powder adsorbent in the fixed bed is easily blown by gas and blocked pipes (Valizadeh et al., 2018). The pellet was more suitable for adsorption with excellent mechanical strength and adsorption performance. A common method is to mold powder by adding a binder. The commonly used binders include CMC (Chen et al., 2016), bentonite (Jo et al., 2021), polyvinylbutyral resin (Qiao et al., 2001) and alumina (Valekar et al., 2017). For CaO-based sorbent pelletization, Manovic and Anthony (2009) considered calcium aluminate cements binder was better than bentonite binder. Rezaei et al. (2015) discovered that the pellet prepared at higher pressure changed porosity and internal gas transmission was poor, which reduced its absorption rate. Costa et al. (2020) found a satisfactory trade-off between the concentration of an organic polyvinyl alcohol binder and one of the hematite-based sorbents in a composite.

AlFu MOFs is a promising adsorbent for CO<sub>2</sub> capture. However, the powder adsorbent is easy to lose and block the pipeline. It is necessary to study the pelletization technique to obtain AlFu MOFs pellet with good mechanical property. In this work, firstly pellets were prepared with different CMC mass and then their

mechanical strength and CO<sub>2</sub> adsorption capacity were evaluated. Secondly, the pellet with 2.5wt% CMC was chosen and the functional group, morphology and pore structure were characterized. Thirdly, to recognize the adsorption process and control factor at different adsorption temperatures and partial pressures, CO<sub>2</sub> adsorption kinetics and rate-limiting kinetics were explored. By studying its adsorption mechanism, sufficient information will be provided to better understand adsorption kinetic characteristics of AIFu MOFs and develop the practical application.

## 2. Materials and methods

### 2.1 Preparation of AIFu pellet

The AIFu MOFs were synthesized by a solvent method at room temperature. Disodium fumarate (7.938 g) and aluminum nitrate nonahydrate (9.303 g) were dissolved in 248 mL deionized water. And then solution was mixed and stirred for 10 min. Next the suspension was filtrated and washed with abundant deionized water. After drying at 100 °C under vacuum for 12 h, the white solid AIFu power was obtained.

Based on the successfully prepared AIFu powder, CMC binder was mixed with powders. Then deionized water was added according to the proportion of 1.5 mL of deionized water per gram of mixture. After stirring, the paste-like mixture was placed into a mold in the atmosphere and dried for 1 h at 80 °C. Finally, cylindrical AIFu adsorbent pellets of 5 mm in diameter and 4 mm in height were prepared, as illustrated in Figure 1(a).

### 2.2 Characterization and CO<sub>2</sub> adsorption experiments

Fourier transform infrared spectroscopy (FTIR) was provided by Fourier transform infrared spectrometer (iS10 Thermo fisher Nicolet, America). The morphologies and microstructure were observed by a Scan Electron Microscope (SEM, SU8020 Hitachi, Japan). The N<sub>2</sub> adsorption-desorption isotherms were measured at 77 K using a BET analyzer (Micromeritics ASAP2460, America). The CO<sub>2</sub> adsorption performance of the AIFu adsorbent was also measured using the thermal gravimetric analyzer (TGA, Netzsch STA 409PC Luxx, Germany). Concerning the adsorption balance time and experimental experience, pellets were heated to 150 °C for about 1 h under N<sub>2</sub> to remove water and other gas impurities before adsorption. The temperature was then reduced to the adsorption temperature and the purge gas was switched to CO<sub>2</sub>. The analyser recorded the mass change during the adsorption.

## 3. Results and discussion

### 3.1 Effect of binder on mechanical strength and CO<sub>2</sub> adsorption performance of AIFu pellet

Figure 1(b) illustrates CO<sub>2</sub> adsorption capacity and mechanical strength of AIFu pellet with various CMC mass. When the CMC mass ratio was 2.5 wt%, the highest CO<sub>2</sub> adsorption capacity was 1.26 mmol/g. The CO<sub>2</sub> adsorption capacity gradually decreased with binder mass increase. The first reason was that the AIFu powder mass in pellet decreased as the binder mass increased. Second, the pores of AIFu were blocked after adding binder. The pore blocking became more serious as the binder mass increased. So both CO<sub>2</sub> adsorption sites and adsorption capacity were reduced. On the contrary, with the rise in binder mass, the mechanical strength of pellet raised from 1.486 MPa at 2.5 wt% to 11.290 MPa at 20 wt%. The pellet mechanical strength and CO<sub>2</sub> adsorption capacity must be taken into account in applications, so the pellet with 2.5wt% CMC was chosen as the target adsorbent to test its performance.

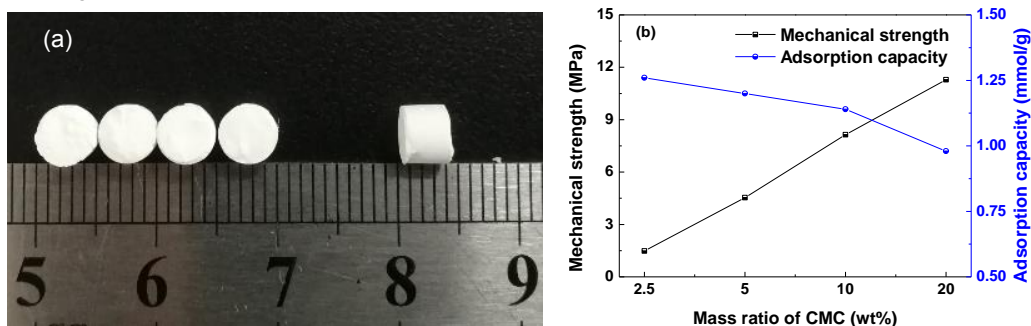


Figure 1: (a) the appearance and (b) mechanical strength of AIFu pellet

### 3.2 Characteristics of AIFu pellet

The SEM figure and FTIR spectra of AIFu pellet are shown in Figure 2. Many small nanoparticles aggregated into large particles of 300–400 nm. The agglomeration and the pellet pore generated a well-developed pore structure. Broadband at approximately  $3,425\text{ cm}^{-1}$  corresponded to the -OH stretching vibration from free water or AIFu. Strong vibration peaks at  $1605\text{ cm}^{-1}$  and  $1,425\text{ cm}^{-1}$  were related to the -COO- asymmetric and symmetric stretching in the fumarate. The multiple bands located within the  $500\text{--}1,200\text{ cm}^{-1}$  were the distinct traits of Al-O vibrations in the framework.

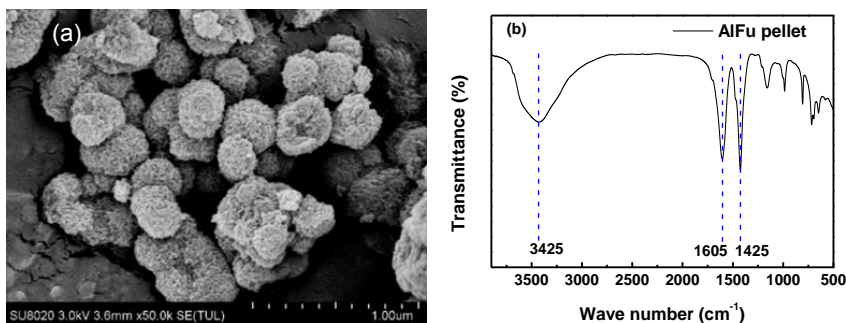


Figure 2: (a) SEM and (b) FTIR figures of AIFu pellet

The  $\text{N}_2$  adsorption-desorption isotherm and pore distribution of AIFu pellet are observed in Figure 3. The shape of isotherm indicated the material had microporous structure. Under extremely low relative pressure, the adsorption amount increased sharply and then became flat. An adsorption-desorption hysteresis loop appeared when the relative partial pressure ( $P/P_0$ ) was 0.5–1.0. The micropore volume was  $0.33\text{ cm}^3/\text{g}$ . The remarkable specific surface area was  $726.06\text{ m}^2/\text{g}$ , which was higher than hollow silica nanospheres  $230.95\text{ m}^2/\text{g}$  (Ding et al., 2019) and hematite-based sorbents  $52\text{ m}^2/\text{g}$  (Costa et al., 2020), but was lower than AIFu MOF  $971\text{ m}^2/\text{g}$  (Coelho et al., 2016).

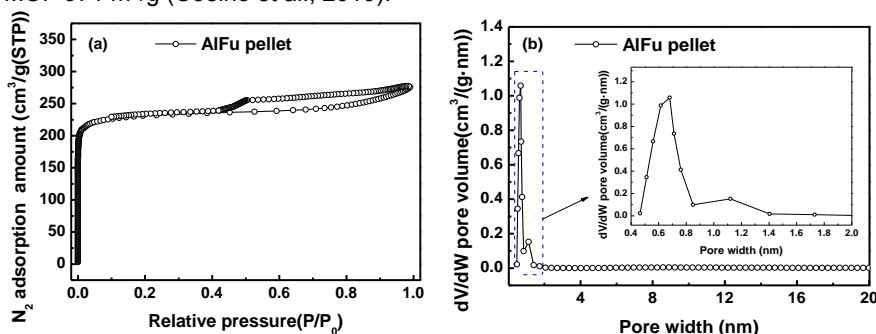


Figure 3: (a)  $\text{N}_2$  adsorption-desorption isotherm and (b) pore distribution of AIFu pellet

### 3.3 $\text{CO}_2$ adsorption kinetics characteristics of AIFu pellets

Pseudo-first and pseudo-second order gas-solid adsorption models are widely used because of the simple description of the adsorption kinetics and the adsorbent-adsorbate interactions. Eq(1) and Eq(2) are the model equations:

$$q_t = q_e(1 - e^{-k_1 t}) \quad (1)$$

$$q_t = \frac{q_e^2 k_2 t}{1 + q_e k_2 t} \quad (2)$$

Considering the influence of  $\text{CO}_2$  partial pressure and temperature on the adsorption, the adsorption process is analyzed by different kinetic models in Figure 4, and the kinetic parameters are shown in Table 1. It could be noticed that the fitting curve obtained by the pseudo-first order model was closer to the experimental result. The non-linear determination coefficient  $R^2$  was 0.98 and was larger than  $R^2$  of the pseudo-second order

model. Therefore, the pseudo-first order kinetic model could better describe the CO<sub>2</sub> adsorption behavior of AIFu pellet. It can be considered as physical adsorption rather than chemical adsorption. With the increase of CO<sub>2</sub> partial pressure, the pseudo-first order adsorption rate constant gradually raised from 0.405 min<sup>-1</sup> (0.3 bar) to 0.784 min<sup>-1</sup> (1.0 bar). However, when the temperature was increased, the intermolecular force dropped as the molecular thermal motion intensified and the amount of CO<sub>2</sub> adsorption decreased. Consequently, the pseudo-first order adsorption rate constant improved slightly.

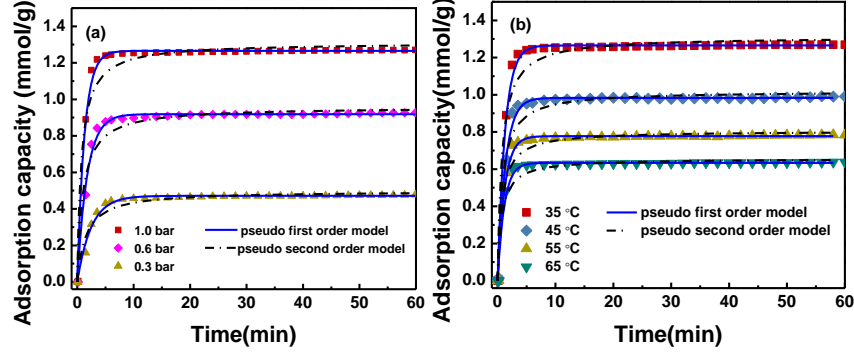


Figure 4: CO<sub>2</sub> adsorption kinetic characteristics of AIFu pellet: (a) different CO<sub>2</sub> partial pressures; (b) different adsorption temperatures

Table 1: Dynamic parameters of pseudo-first order and pseudo-second order models under different adsorption conditions

Adsorption condition	q <sub>exp</sub>	Pseudo-first order model			Pseudo-second order model		
		q <sub>cal</sub>	k <sub>1</sub>	R <sup>2</sup>	q <sub>cal</sub>	k <sub>2</sub>	R <sup>2</sup>
35 °C, 0.3 bar	0.47	0.472	0.405	0.990	0.498	1.336	0.968
35 °C, 0.6 bar	0.92	0.919	0.572	0.991	0.958	1.044	0.969
35 °C, 1.0 bar	1.26	1.265	0.784	0.989	1.311	1.047	0.962
45 °C, 1.0 bar	0.98	0.983	0.750	0.990	1.020	1.295	0.965
55 °C, 1.0 bar	0.78	0.777	0.833	0.987	0.806	1.766	0.960
65 °C, 1.0 bar	0.63	0.634	0.873	0.985	0.656	2.268	0.956

### 3.4 Rate-limiting kinetics characteristics of AIFu pellet

Although the pseudo-first order kinetic model described the CO<sub>2</sub> adsorption behavior, the limiting adsorption rate factors were still unclear. Thus the Boyd film diffusion model, inter-particle diffusion model and intra-particle diffusion model were selected to evaluate the limiting factors.

The Boyd film diffusion model is a single resistance model assuming that the main resistance is the gas film surrounding the adsorbent. It can be used to estimate whether the adsorption rate is affected by film diffusion resistance with B<sub>i</sub> curve. The model is as follow:

$$F = 1 - \frac{6}{\pi^2} \sum_{n=1}^{\infty} \frac{1}{n^2} \exp(-n^2 B_i) \quad (3)$$

For F > 0.85,

$$B_i = -0.4977 - \ln(1 - F) \quad (4)$$

For F < 0.85,

$$B_i = -(\sqrt{\pi} - \sqrt{\pi - (\frac{\pi^2 F}{3})})^2 \quad (5)$$

The inter-particle diffusion model was used to predict the inter-particle diffusion behavior. The model is described as:

$$\frac{q_t}{q_e} = 1 - \frac{6}{\pi^2} \sum_{n=1}^{\infty} \frac{1}{n^2} \exp\left(-\frac{n^2 \pi^2 D_c t}{r_p^2}\right) \quad (6)$$

When the fractional adsorption capacity ( $q_t/q_e$ ) is greater than 70%, Eq(6) can be simplified as:

$$1 - \frac{q_t}{q_e} \approx \frac{6}{\pi^2} \exp\left(-\frac{\pi^2 D_c t}{r_p^2}\right) \quad (7)$$

If the adsorbent has plenty of pore structure or pores are mainly microporous, CO<sub>2</sub> adsorption process may be determined by intra-particle diffusion resistance. The expression of the intra-particle diffusion model is:

$$q_t = k_{id} t^{1/2} + C \quad (8)$$

The adsorption performance at 35 °C and various CO<sub>2</sub> partial pressures are employed to rate-limiting kinetic analysis in Figure 5. Figure 5(a) showed the curves of  $B_t$  versus time in film diffusion model. The curves all passed through the origin but were not linear. Hence, the pellet CO<sub>2</sub> adsorption was affected by the film diffusion resistance. Details of the inter-particle diffusion model are displayed in Figure 5(b) and Table 2. The curves of  $\ln(1-q_t/q_e)$  also showed no linearity. The intercept of the three fitting straight lines was in poor agreement with measured value. Therefore, the inter-particle diffusion resistance was not the main factor limiting the adsorption rate. In addition, intra-particle diffusion model was also used to analyze the adsorption process, as seen in Figure 5(c). It was evident that all the adsorption curves exhibited three stages, including slow growth, rapid growth and eventually unchanged. This indicated there was another diffusion resistance in the adsorption. So inter-particle diffusion was not the main factor determining the adsorption rate of AIFu pellets but both film diffusion and intra-particle diffusion.

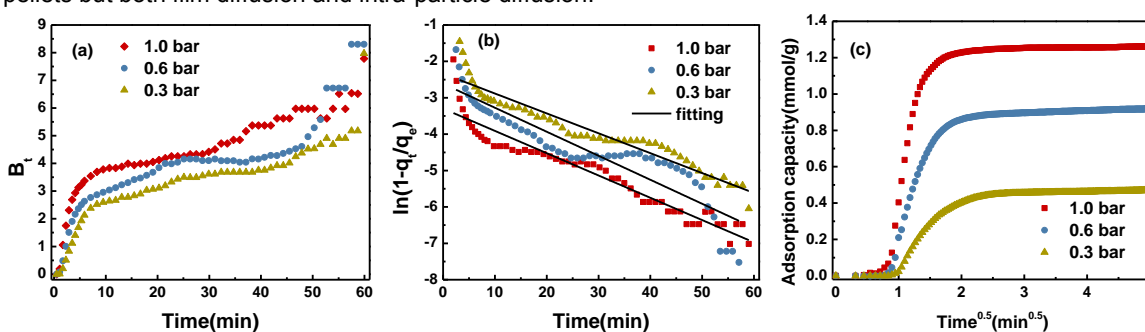


Figure 5: Rate-limiting kinetic characteristics of AIFu pellet: (a) film diffusion model, (b) inter-particle diffusion model and (c) intra-particle diffusion model

Table 2: Linear fitting parameters of intra-particle diffusion model of AIFu pellet

CO <sub>2</sub> partial pressure	Slope	Intercept	R <sup>2</sup>
0.3 bar	-0.054	-2.34	0.92
0.6 bar	-0.066	-2.61	0.84
1.0 bar	-0.061	-3.30	0.92

#### 4. Conclusions

Porous AIFu MOF pellet had been synthesized rapidly with CMC binder base on powder. By exploring the influence of CMC mass on the pellet mechanical strength and adsorption capacity, pellet with 2.5wt% CMC was chosen to investigate adsorption performance by apparent kinetic models and rate-limiting models. The results showed that the CO<sub>2</sub> adsorption capacity was increased with lower adsorption temperature and higher CO<sub>2</sub> partial pressure. The optimum adsorption capacity was 1.26 mmol/g at 35 °C and 1.0 bar. The pseudo-first order kinetic model can better describe the CO<sub>2</sub> physical adsorption behavior of AIFu pellet. The rate-limiting kinetic analysis revealed that the CO<sub>2</sub> adsorption rate was determined by film diffusion and intra-particle diffusion. In future research it is necessary to explore the recycling stability performance and the adsorption thermodynamic characteristics of the adsorbent.

## Nomenclature

$B_t$ – mathematical function of $F$ , -	$q_{cal}$ – adsorption capacity by kinetic model, mmol/g
$C$ – intercept of curve, -	$q_e$ – adsorption capacity at adsorption balance, mmol/g
$D_c$ – diffusion rate, $m^2/s$	$q_{exp}$ – adsorption capacity by experiment, mmol/g
$F$ – fractional adsorption capacity at any time ( $F=q_t/q_e$ ), -	$q_t$ – adsorption capacity at any time, mmol/g
$k_1$ – adsorption rate constant for the pseudo-first order model, $min^{-1}$	$R^2$ - non-linear determination coefficient, -
$k_2$ – adsorption rate constant for the pseudo-second order model, $min^{-1}$	$r_p$ – radius of pellet, m
$k_{id}$ – intra-particle diffusion rate constant, $mol/(kg \cdot min^{-0.5})$	$t$ – adsorption time, s

## Acknowledgements

This work was supported by National Natural Science Foundation of China (No. 51876013), Innovative research group project of National Natural Science Foundation of China (No. 52021004), and the Venture & Innovation Support Program for Chongqing Overseas Returnees (No. CX2018054).

## References

- Chen L., Ding Y.D., Zhun X., Liao Q., Song G., Wang H., 2016, Synthesis of MgO pellets with high specific surface area and its CO<sub>2</sub> adsorption property, *Journal of Engineering Thermophysics*, 37, 1243-1248.
- Coelho J.A., Ribeiro A.M., Ferreira A.F.P., Lucena S.M.P., Rodrigues A.E., Azevedo D.C.S., 2016, Stability of an Al-Fumarate MOF and its potential for CO<sub>2</sub> capture from wet stream, *Industrial and Engineering Chemistry Research*, 55, 2134-2343.
- Costa C., Cornacchia M., Pagliero M., Fabiano B., Vocciante M., Reverberi A.P., 2020, Hydrogen sulfide adsorption by iron oxides and their polymer composites: a case-study application to biogas purification, *Materials*, 13, 4725.
- Ding Y.D., Guo L.H., Li X.Q., Liao Q., Zhu X., Wang H., 2019, Synthesis and CO<sub>2</sub> absorption of anhydrous colloidal suspension based on hollow silica nanospheres, *Chemical Engineering Transaction*, 76, 1051-1056.
- Dundar E., Bozbiyik, B., Perre S.V.D., Maurin G., Denayer J.F.M., 2017, Modeling of adsorption thermodynamics of linear and branched alkanes in the aluminum fumarate metal organic framework, *The Journal of Physical Chemistry*, 121, 20287-20295.
- Jeremias F., Fröhlich D., Janiak C., Henninger S.K., 2014, Advancement of sorption-based heat transformation by a metal coating of highly-stable, hydrophilic aluminium fumarate MOF, *RSC Advances*, 4, 24073-24082.
- Jo J.Y., Choi J.H., Tsang Y.F., Baek K., 2021, Pelletized adsorbent of alum sludge and bentonite for removal of arsenic, *Environmental Pollution*, 277, 116747.
- Karmakar S., Dechnik J., Janiak C., De S., 2016, Aluminium fumarate metal-organic framework: A super adsorbent for fluoride from water, *Journal of Hazardous Materials*, 30, 10-20.
- Manovic V., Anthony W.J., 2009, Screening of binders for pelletization of CaO-based sorbents for CO<sub>2</sub> capture, *Energy and Fuels*, 23, 4797-4804.
- Qiao W.M., Korai Y., Mochida I., Hori Y., Maeda T., 2001, Preparation of an activated carbon artifact: factors influencing strength when using a thermoplastic polymer as binder, *Carbon*, 39, 2355-2368.
- Rezaei F., Sakwa-Novak M.A., Bali S., Duncanson D.M., Jones C.W., 2015, Shaping amine-based solid CO<sub>2</sub> adsorbents: effects of pelletization pressure on the physical and chemical properties, 204, 34-42.
- Sadiq M.M., Rubio-Martinez M., Zadehahmadi F., Suzuki K., Hill M.R., 2018, Magnetic framework composites for low concentration methane capture, *Industrial and Engineering Chemistry Research*, 57, 6040-6047.
- Teo H.W.B., Chakraborty A., Kitagawa Y., Kayal S., 2017, Experimental study of isotherms and kinetics for adsorption of water on Aluminium Fumarate, *International Journal of Heat and Mass Transfer*, 114, 621-627.
- Valekar A.H., Cho K.H., Lee J.S., Yoon J.W., Hwang Y.K., Lee S.G., Cho S.J., Chang J.S., 2017, Shaping of porous metal-organic framework granules using mesoporous  $\gamma$ -alumina as a binder, *RSC Advances*, 7, 55767-55777.
- Valizadeh B., Nguyen T.N., Stylianou K.C., 2018, Shape engineering of metal-organic frameworks, *Polyhedron*, 145, 1-15.